

# Increased glacier melt enhances future extreme floods in the southern Tibetan Plateau

He SUN<sup>a,\*</sup>, Tan-Dong YAO<sup>a</sup>, Feng-Ge SU<sup>a</sup>, Tinghai OU<sup>b</sup>, Zhihua HE<sup>c</sup>, Guoqiang TANG<sup>d</sup>,  
Deliang CHEN<sup>b</sup>

<sup>a</sup> State Key Laboratory of Tibetan Plateau Earth System, Environment and Resources (TPESER),

Institute of Tibetan Plateau Research, Chinese Academy of Sciences, Beijing 100101, China

<sup>b</sup> Regional Climate Group, Department of Earth Sciences, University of Gothenburg, Gothenburg 405 30, Sweden

<sup>c</sup> Centre for Hydrology, University of Saskatchewan, Saskatoon S7N 1K2, Canada

<sup>d</sup> Climate and Global Dynamics, National Center for Atmospheric Research, Boulder CO 80307, USA

Received 10 September 2023; revised 25 October 2023; accepted 4 January 2024

## Abstract

Mountainous areas are of special hydrological concern because topography and atmospheric conditions can result in large and sudden floods, posing serious risks to water-related safety in neighbouring countries. The Yarlung Zangbo (YZ) River basin is the largest river basin on the Tibetan Plateau (TP), but how floods will discharge in this basin and how the role of glacier melt in floods will change throughout the 21st-century under shared socioeconomic pathways scenarios (SSP2-4.5 and SSP5-8.5) remain unclear. Here, we comprehensively address this scientific question based on a well-validated large-scale glacier-hydrology model. The results indicate that extreme floods was projected to increase in the YZ basin, and was mainly reflected in increased duration (4–10 d per decade) and intensity (153–985 m<sup>3</sup> s<sup>-1</sup> per decade). Glacier runoff was projected to increase (2–30 mm per decade) throughout the 21st-century, but there was also a noticeable decrease or deceleration in glacier runoff growth in the late first half of the century under the SSP2-4.5, and in the latter half of the century under the SSP5-8.5. Glacier melt was projected to enhance the duration (12%–23%) and intensity (15%–21%) of extreme floods under both SSPs, which would aggravate the impact of future floods on the socioeconomics of the YZ basin. This effect was gradually overwhelmed by precipitation-induced floods from glacier areas to YZ outlet. This study takes the YZ basin as a projection framework example to help enrich the understanding of future flood hazards in basins affected by rainfall- or meltwater across the TP, and to help policy-makers and water managers develop future plans.

## 1. Introduction

Changes in the extreme hydrological events (floods and droughts) are one of the most significant consequences of climate change (Belloni et al., 2021). Extreme floods, one of the deadliest global natural hazards, have impacts on almost two billion people globally during 1998–2017 (AghaKouchak et al., 2020). Changes in the future extreme floods and their influences on socioeconomics have received extensive

attention at both regional (Su et al., 2022; Wang et al., 2024) and global scales (Boulangue et al., 2021; Xiao et al., 2023).

Mountainous areas on the Tibetan Plateau (TP) are of special concern in a hydrological context because their complex terrain and atmospheric conditions may cause large floods. The southern TP plays a crucial role in supplying transboundary rivers, including the Indus, Ganges, and Brahmaputra Rivers, and serves as a water source for nearly one billion individuals (Lutz et al., 2022). This region and its adjacent plains are highly flood-prone, which poses serious risks to safety in neighbouring countries. Zhou (2020) suggested the flood peaks exhibited an increased trend in the southern Tibetan Plateau, and the rate changed from about 10% per decade (1961–1990) to 15% per decade (1991–2017). Su et al. (2022) suggested that extensive

\* Corresponding author.

E-mail address: [sunhe@itpcas.ac.cn](mailto:sunhe@itpcas.ac.cn) (SUN H.).

Peer review under responsibility of National Climate Center (China Meteorological Administration).

<https://doi.org/10.1016/j.accre.2024.01.003>

1674-9278/© 2024 The Authors. Publishing services by Elsevier B.V. on behalf of KeAi Communications Co. Ltd. This is an open access article under the CC BY-NC-ND license (<http://creativecommons.org/licenses/by-nc-nd/4.0/>).

glacier and snow coverage make it very difficult to accurately estimate or forecast the future extreme flood changes in the TP. Furthermore, an absence of dependable hydrometeorological information and large differences in downscaling approaches have hindered a comprehensive understanding of the future flow regimes and extremes on the TP (Su et al., 2022).

The aforementioned issues are typical of the Yarlung Zangbo (YZ, also referred to as the upper Brahmaputra) River of the southern TP, limiting our understanding of changes in extreme floods in this basin. The YZ basin, the biggest river basin of the TP, not only acts as the primary freshwater supply but also the main agricultural center of the TP. Over the past few decades, the warming trend across the YZ basin has been stronger than the global average (Sun and Su, 2020). Under a warming climate, the YZ basin has experienced many climate-induced changes, including glacier retreat (Yao et al., 2012) and glacial lake outburst floods (An et al., 2021), threatening the safety and livelihoods of local people. Past research has emphasized the significance of precipitation and glacier melting in determining historical runoff generation and future runoff changes at annual and seasonal timescales in the YZ basin (Su et al., 2016; Sun and Su, 2020; Wang et al., 2021). However, the ways in which flood discharges will evolve throughout the 21st-century under climate change are insufficiently recognized over the YZ basin. Shao et al. (2023) suggested that the YZ basin might become wetter with increasing extreme floods. Wijngaard et al. (2017) suggested that future flood hazards were likely resulted from projected precipitation increases in the YZ basin. Yang et al. (2022) suggested floods in the YZ basin were related to storms. In addition, glaciers would experience irregular, frequent, and sudden advances (surges) that pose an increasing threat of flooding throughout the TP region. However, the YZ basin contains approximately 10% of the TP's entire glacier coverage, which is higher than that in other monsoon-dominated basins of the TP. There is limited relevant knowledge regarding the contribution of glacier melting to flood timing and intensity in the YZ basin, especially in its downstream region which contains substantial areas of glaciers (approximately 65% of the total glacial area in the YZ basin). It is of both scientific and public interest to understand how and why future flood frequency and intensity will change.

Here, we took the YZ basin as a projection framework example to address two scientific questions that are crucial for understanding future floods on the TP: 1) How will the frequency, duration, and intensity of extreme floods change in the 21st-century? 2) How important is glacier melt to extreme floods in the YZ basin? We comprehensively addressed the above questions in the YZ basin by a process-based glacier-hydrology model and 10 global climate models (GCMs) from the latest release of the Coupled Model Intercomparison Project Phase 6 (CMIP6). Based on these scientific questions, we also tried to investigate the relationship of glacier melting in flood risks with socioeconomic (population and gross domestic product) exposure in the YZ basin. We wish to close the

knowledge gap on this topic in the YZ basin, aiming to improve our understanding of future extreme flood changes on the TP, and to help policy makers and water managers develop future strategies.

## 2. Study area

The YZ basin was divided into the Nuxia (NX, 201,548 km<sup>2</sup>) and a basin between Nuxia and Pasighat outlet (NX-BXK, 51,507 km<sup>2</sup>; Fig. 1). The YZ basin was projected to be wetter and warmer in the future (Table A1). The runoff of the YZ basin is dominated by monsoon-induced precipitation (Sun and Su, 2020). Along with increasing precipitation and temperature (Fig. A1), total runoff will increase by 7–34 mm per edcade under SSP2-4.5, and 27–101 mm per edcade under SSP5-8.5 for 2015–2100 in the YZ (Fig. 1), which is mostly due to increased precipitation-induced runoff. In addition to precipitation, glacier runoff also influences the runoff regimes in the YZ basin. The YZ basin contains approximately 10 % (8273 km<sup>2</sup>) of the TP's total glacier area. The largest glacier coverage of the YZ lies in the NX-BXK sub-basin (10.2 %), and glacier runoff contributes 13 % and 19 % of total runoff in the NX and NX-BXK, respectively.

## 3. Materials and methods

### 3.1. Glacier-hydrology model

The Variable Infiltration Capacity (VIC) (Liang et al., 1994) hydrological model coupled with a degree-day glacier melt algorithm (Hock, 2003) (termed as VIC-Glacier) were used to simulate future extreme floods in the YZ basin. As a semi-distributed macroscale hydrological model, it solves full water and energy balances within the grid cell. The VIC-Glacier model has previously been used in runoff simulations and predictions in the TP (Zhang et al., 2013; Sun et al., 2021, 2022).

Here, the modeling framework at a  $1/12^\circ \times 1/12^\circ$  (approximately 10 km  $\times$  10 km) spatial resolution and a 3-h time step was adopted from Sun and Su (2020). The required forcing input data for the VIC-Glacier model included daily meteorological forcing data (precipitation, maximum and minimum temperatures, and wind speeds) with a spatial resolution of 10 km  $\times$  10 km for 1961–2020, which was adopted from Sun et al. (2022).

Observed streamflow and glacier mass balance were applied to calibrate and validate the model. The Nash-Sutcliffe efficiency (NSE), relative bias (RB, %), and correlation coefficient (CC), were applied to assess the performance of the hydrological model. The trial-and-error method was used for the optimization process in order to achieve the least bias between simulations and observations against the corresponding criteria. First, initial values of Degree-Day factor (DDF) parameters (6.5–11.0 mm °C<sup>-1</sup> d<sup>-1</sup>) in the glacier model related to glacier and snowmelt were adopted from Sun

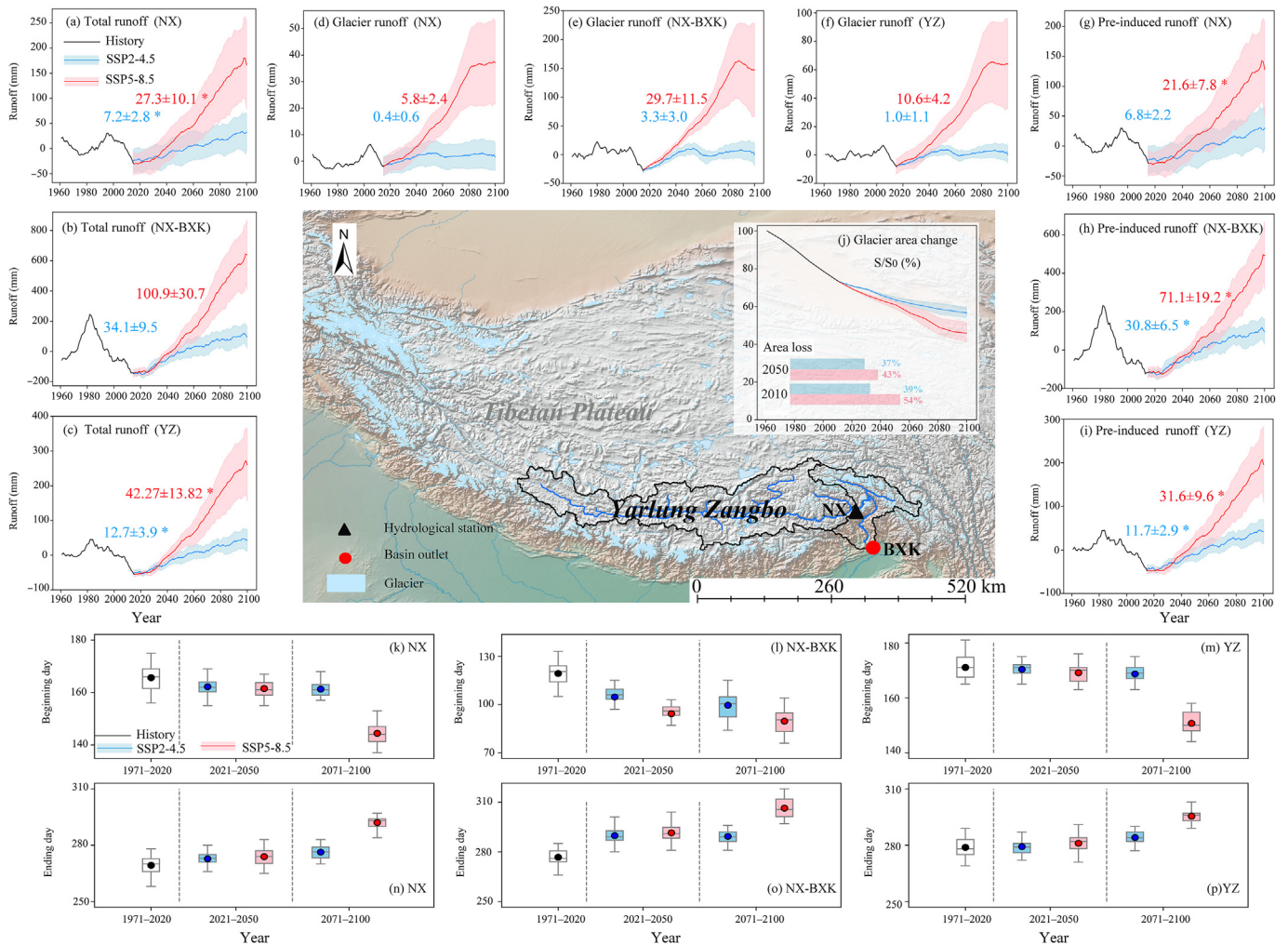


Fig. 1. (a–i) Simulated total runoff, precipitation-induced (Pre-induced) runoff, and glacier runoff in the YZ basin and its NX and NX-BXK sub-basins with 30-year moving windows from 1961 to 2100, (j) simulated evolution of glacier area relative to initial area ( $S/S_0$ ) from 1961 to 2100 in the YZ basin (Mean glacier area losses ( $1-S/S_0$ ) in 2050 and 2100 are indicated). The solid lines for the projection (2015–2100) indicate the ensemble means of all transient simulations for each year. Shadings denote the standard deviation of 10 hydrological model runs driven by different climate models. The numbers in each panel are the tendency of runoff (mm per decade) for 2021–2100 for each SSP, respectively) simulated beginning (k–m) and ending (n–p) day of glacier runoff with three 30-year windows including the reference (1971–2000) and two future periods (2021–2050 and 2071–2100) based on the ensemble mean of 10 transient runs for each SSP. Asterisks indicate the 0.05 significance level.

and Su (2020). Second, the VIC-related model parameters, mostly the infiltration shape parameter ( $B_{inf}$ ) and second soil layers (D2), were calibrated and validated with streamflow observations. The VIC-Glacier model captured well the magnitudes and patterns of observed runoff at daily (Fig. 2a) scale for 1971–1980 in the NX hydrological station (Fig. 1), with NSEs of 0.91–0.96 and RBs of  $-2\%$  to  $-1\%$ . Due to the lack of daily and monthly observed streamflow estimates, annual observation for 2015–2019 was used to validate the model performance in Motuo (MT, Fig. 1) hydrological station. The closed agreements between the observed and simulated runoff were seen at the annual scale in the MT (Fig. 2b), with a CC of 0.83. After the careful calibration and validation, the final values of D1, D2 and  $B_{inf}$  for each grid cell were set to 0.1, 0.8–1.0, and 0.2 m in these two sub-basins, respectively.

### 3.2. GCM data, downscaling and bias-correction

To generate the forcing inputs for the hydrological model in the YZ basin, the monthly estimates of precipitation and temperature from 10 GCMs (Table 1, <https://esgf-node.llnl.gov>) for the period 2015–2100 in the CMIP6 (Eyring et al., 2016) were utilized. These estimates were selected based on their ability to replicate the observed seasonal pattern and their minimal deviation from the observations among 18 models (Li et al., 2021). The climate projections in the YZ basin throughout the 21st century were investigated by selecting the SSP2-4.5 and SSP5-8.5 scenarios in the CMIP6. Using the newly reconstructed reference data from 1961 to 2014 (Sun et al., 2022), the raw monthly GCM outputs for 2015–2100 underwent statistical downscaling and bias correction through the widely utilized bias corrected spatial disaggregation (BCSD) method (Wood, 2002).

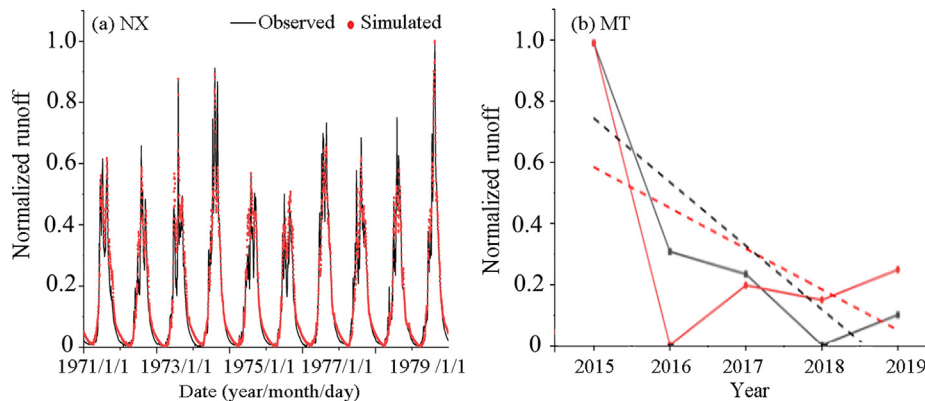


Fig. 2. (a) Daily observed and simulated streamflow for 1971–1980 at Nuxia (NX) hydrological station, and (b) observed and simulated annual runoff for 2015–2019 at Motuo (MT) hydrological station.

Table 1

Details of the 10 CMIP6 global climate models used in the precipitation and temperature projections for the period 2015–2100.

Number	Model	Institute ID	Region/ Country	Atmosphere resolution (longitude × latitude)
1	BCC-CSM2-MR	BCC	China	2.8125° × 2.7906°
2	CAMS-CSM1	CAMS	China	1.1250° × 1.1215°
3	CNRM-CM6	CNRM	France	1.4063° × 1.4008°
4	CNRM-ESM2			
5	EC-Earth3	EC-Earth_ Cons	Europe	1.1250° × 1.1215°
6	EC-Earth3-Veg	EC-Earth_ Cons	Europe	1.1250° × 1.1215°
7	IPSL-CM6A-LR	IPSL	France	3.7500° × 1.8947°
8	MRI-ESM2-0	MRI	Japan	1.1250° × 1.1215°
9	MIROC6	MIROC	Japan	1.4063° × 1.4008°
10	UKESM1-0-LL	MOHC	UK	1.1250° × 1.8750°

This method had demonstrated consistent and realistic performances compared to historical climate records (Su et al., 2022; Thrasher et al., 2012; Wood et al., 2004).

Initially, the GCMs underwent bias correction by applying quantile mapping relationships between the historical reference data and the simulated historical precipitation and temperature data from all GCMs. This correction was performed for the overlapping period (1961–2014) at a resolution of  $1^\circ \times 1^\circ$  in the YZ basin. Furthermore, a spatial–temporal disaggregation was conducted by resampling the monthly gridded observed precipitation and temperature data at VIC-Glacier resolution ( $1/12^\circ \times 1/12^\circ$ ). In the end, the monthly data was temporarily broken down into daily intervals by sampling the daily historical data based on the monthly averages of the locally adjusted data for the years 2015–2100. Following this procedure, the VIC-Glacier model utilized the daily transient climate projections from 20 different scenarios (10 GCMs × 2 SSPs) to generate uninterrupted projections.

### 3.3. Extreme flood indices

Future changes in extreme floods were assessed by analysing changes in frequency, duration and intensity.

Conceptualization of the flood frequency, duration and intensity were shown in Fig. 3j.

First, we determined a flood threshold by the 95% exceedance frequency of flow duration curves (FDCs) (Cigizoglu and Bayazit, 2000) of the daily streamflow in the historical period (1961–2014), which was commonly used in the analysis of flood frequencies (Hoang et al., 2016; Lutz et al., 2016; Sun et al., 2021). The occurrence of extreme floods was from the onset when daily streamflow exceeded this extreme flood threshold to the end when daily streamflow was below this threshold. The annual flood frequency (Freq) was the number of flood occurrences within a year (Table 2). The annual maximum consecutive flood days (CFD), the maximum consecutive days within a year when daily streamflow remains above the extreme flood threshold, were calculated for the extreme flood duration (Table 2). The annual maximum daily discharge (AMD) was calculated for the extreme flood intensity. In addition, we also used it to measure flood intensity with return periods of 20, 50, and 100 years (Hirabayashi et al., 2013).

Precipitation-induced runoff and glacier melt were the most important factors responsible for streamflow changes in the YZ basin. Here, the consecutive 5-d precipitation (Rx5day) and total precipitation amounts were calculated when daily precipitation estimates were greater than 95th percentile (R95P) (Table 2). The difference between the simulated annual maximum daily discharge with and without glacier runoff was calculated to analyse the role of glacier melt in extreme floods. In addition, we designed the beginning day (BD) and ending day (ED) to analyse the duration of glacier runoff. The BD (ED) of glacier runoff was defined as the first (last) day of the first (last) 5 consecutive days when daily glacier runoff exceeded a threshold, which was in the 95th percentile of daily glacier runoff during May–September in the historical period (1961–2014) for each sub-basin.

The implications of the projected changes in future floods for human society could be measured by the populations and gross domestic product (GDP) (Hirabayashi et al., 2013). The population exposed to flooding was calculated by overlaying the simulated inundation area onto a gridded population dataset (Hirabayashi et al., 2013). It was calculated as

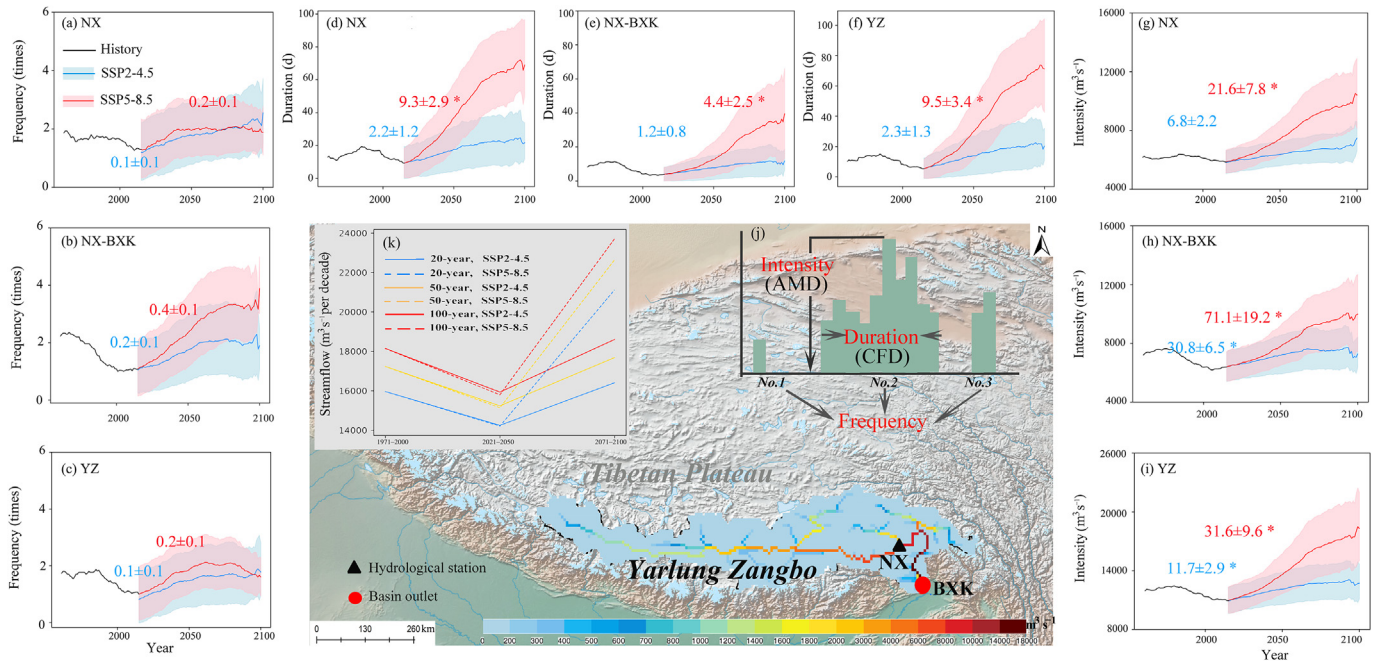


Fig. 3. (a–i) Simulated annual frequency, duration and intensity of floods in the upstream region of the Nuxia (NX) hydrological station and downstream region between NX and the Pasighat (BXX) outlet (NX-BXX) of the Yarlung Zangbo (YZ) river basin with 30-year moving windows from 1971 to 2100 (The solid lines for the projection period (2015–2100) indicate the ensemble means of 10 transient simulations for each year. Shadings denote the standard deviation of 10 hydrological model runs driven by different climate models under each SSP. (j) conceptualization of the flood frequency, flood duration that is defined by annual maximum consecutive flood days (CFD), and intensity of flood that is defined by annual maximum daily discharge (AMD), (k) the AMD corresponding to 20, 50 and 100-year return periods under each SSP with three 30-year windows including the reference (1971–2000) and two future periods (2021–2050 and 2071–2100) based on the ensemble mean of 10 transient runs for each SSP (The spatial pattern of the AMD based on the ensemble mean of 10 transient runs for SSP5-8.5 are shown at the bottom. Asterisks indicate the 0.05 significant level).

Table 2  
Details of statistical extreme indices.

Index	Descriptive	Definition	Unit
Freq	Extreme flood frequency	Annual number of flood occurrences when daily discharge > 95th percentile	times
CFD	Extreme flood duration	Consecutive days when daily discharge > 95th percentile	d
AMD	Extreme flood intensity	Annual maximum daily discharge	$\text{m}^3 \text{s}^{-1}$
Rx5day	Extreme precipitation	Annual maximum consecutive five day precipitation	mm
R95P	Extreme precipitation	Annual total precipitation from daily precipitation > 95th percentile	mm

$$E = P \times f_{\text{flood}} \quad (1)$$

where,  $E$  is the exposure,  $f_{\text{flood}}$  is the simulated AMD, and  $P$  is the population number. The GDP exposed to flooding was also calculated by Eq. 1, where  $P$  was replaced by GDP. The future population dataset was from <https://sedac.ciesin.columbia.edu/data/set/popdynamics-1-km-downscaled-pop-base-year-projection-ssp-2000-2100-rev01>, and the future GDP dataset was from <https://www.zenodo.org/record/5880037>.

## 4. Results

### 4.1. Change in extreme floods

Under an ongoing and expected continued wetting (23–62 mm per decade) and warming (0.4–0.8 °C per decade) trend throughout the 21st-century in the YZ (Table A1), general declines in the historical flood extremes were

consistently projected to change to a strong increase throughout the 21st-century in all basins under both SSPs (Fig. 3a–i). This result was consistent with the annual change in total runoff that was dominated by increased precipitation-induced runoff (Fig. 1).

The increased extreme floods were mainly reflected in their duration and intensity. Extreme flood duration was projected to increase 1–2 d per decade and 4–10 d per decade in all basins for or SSP2-4.5 and SSP5-8.5, respectively (Fig. 3d–f) for 2021–2100, with greater increase rates (8–12 d per decade) in the latter half of the century for the SSP5-8.5. Compared to 1971–2000, flood duration was estimated to rise by 5%–58% under SSP2-4.5 and by 146%–343% under SSP5-8.5 during 2071–2100, respectively (Table A2). Flood intensity was projected to increase (153–985  $\text{m}^3 \text{s}^{-1}$  per decade) for 2021–2100 in all basins under both SSPs (Fig. 3). The same direction of change in flood intensity at different return periods occurred in the YZ basin (Fig. 3k). Relative to

1971–2000, multi-model means of the 2071–2100 daily maximum discharge were projected to increase by 3%–50% for the 20-year occurrence interval, 4%–58% for the 50-year occurrence interval and 6%–60% for the 100-year occurrence interval in the YZ basin under both the SSPs (Fig. 3k). The change in flood frequency remained almost stable, which was projected to increase less than 1-in-10-year under both the SSPs (Fig. 3).

Although extreme floods were projected to increase, regional differences in flood characteristics occurred between the NX and NX-BXK sub-basins of the YZ basin. The increased rates of flood frequency and intensity for 2021–2100 in the NX-BXK were higher than those in the NX, but the increased rate of flood duration (1–4 d per decade) in the NX-BXK was lower than that in the NX (2–9 d per decade; Fig. 3). This suggests that extreme flooding in the NX-BXK indicated higher intensities and frequencies, and shorter durations, while the opposite was true in the NX sub-basin.

The daily maximum discharge during June–September was mostly affected by monsoon rainfall for the YZ basin. The Rx5Day and R95P showed increasing trends throughout the 21st-century under two SSPs in the YZ and its two sub-basins (Fig. 4; Table A3). The increased rates of the Rx5Day and R95P for 2021–2100 in the NX-BXK (1.6–3.7 mm per decade and 15.5–41.4 mm per decade) were higher than those in the NX (0.1–1.3 mm per decade and 4.8–19.4 mm per decade), which were consistent with changes in flood frequency and intensity (Fig. 3). Relative to 1971–2000, multi-model means of the 2071–2100 Rx5day were projected to increase by 3%–4% in each SSP in 2021–2050, and 5%–21% in 2071–2100 in the NX basin. However, it was projected to decrease by 2%–3% in each

SSP in 2021–2050, and increase by 7%–19% in 2071–2100 in the NX-BXK sub-basin (Fig. 4; Table A3). The change of the R95P was similar to the Rx5Day in these two sub-basins, and showed a high consistency with flood intensity ( $CC > 0.9$ ,  $p < 0.05$ ) in the NX and NX-BXK sub-basins, suggesting that extreme precipitation was the primary climatic factor driving the increase in future extreme flood changes. As a result of different changes of the Rx5Day and R95P, multi-model means of the 2071–2100 Rx5day were projected to increase by 2%–20% in each SSP, and the R95P was projected to increase by 27%–111% under the SSP5-8.5 in the YZ basin (Fig. 4; Table A3).

#### 4.2. Role of glacier melt in extreme flood changes

Glacier melt was also an important influence on changes in extreme floods in glacierized regions (Su et al., 2022). Glacier runoff was projected to increase (2–30 mm per decade; Fig. 1d–f) throughout the 21st-century, but there was also a general fall or slowing growth in the late first half of the century under SSP2-4.5, and in the second half under SSP5-8.5 (Fig. 1d–f), associated with a shrinking area of glaciers (Fig. 1j) and warming rate reduction during those periods. With glacier runoff increasing, relative to 1971–2000, the beginning day of glacier melt was projected to earlier, and the ending day was later for near and long term future periods under both SSPs in the YZ (Fig. 1k–p), suggesting that the increased duration of glacier melt. In addition, glacier runoff changes in the NX-BXK were more sensitive to climate changes than those in the NX, with faster increasing rates and earlier beginning days, mostly due to larger glacier coverage.

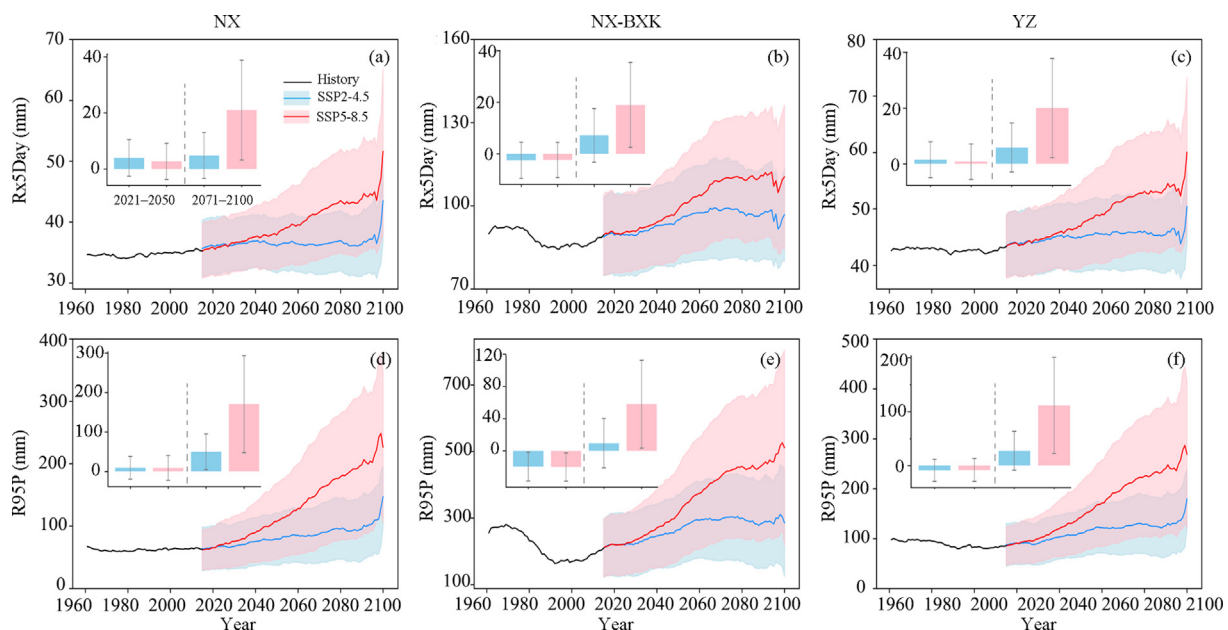


Fig. 4. Simulated Rx5Day and R95P in the YZ basin and its NX and NX-BXK sub-basins with 30-year moving windows from 1961 to 2100 under each SSP (Mean annual changes of extreme precipitation in near future (2021–2050) and far future (2071–2100) relative to the reference period (1971–2000) under each SSP are indicated).

The increased magnitude and duration of glacier melt enhanced its effect on extreme floods throughout the 21st-century (Fig. 5). Glacier melt was projected to contribute of 15%–21% to the annual maximum discharge under both SSPs in the YZ basin, and the contribution was projected to increase from 1971 to 2000 to 2071–2100 under the SSP5-8.5 (Fig. 5g–i). The effect of glaciers on flood intensity was stronger in the SSP5-8.5 than in the SSP2-4.5 during 2071–2100, mostly due to the general decline of glacier runoff under the SSP2-4.5 (Fig. 1). In addition to the intensity, the effect of glacier melt on flood duration was projected to increase in the YZ basin (Fig. 6), which enhanced the flow duration curves (FDCs) from precipitation-induced discharge during flood events (exceedance probability of >95 %). For example, for precipitation-induced runoff, historical peak flows higher than  $8000 \text{ m}^3 \text{ s}^{-1}$  typically occur in extreme flood events, whereas it decreases to 81 % of the total runoff when

supplemented by glacier meltwater (Fig. 6c). The effect of glacier melt on extreme floods was predicted to be stronger in the NX-BXK than in the NX, with a higher reduction in the NX-BXK (79%–81%). The effect of glacier runoff on the duration of extreme floods increased in the latter half of the 21st century in all basins under both SSPs, with an exceedance frequency of 77%–83% (Fig. 6g–i, m–o), owing to large increases in glacier runoff (Fig. 1). Compared with flood intensity and duration, glacier melt played weaker roles on the beginning day of extreme floods (Fig. 5a–f).

Flooding can severely damage socioeconomic development. The mean annual maximum daily discharges were higher in the middle and downstream YZ basin (Fig. 7), where the Lhasa, Rikaze and Linzhi contain more than 70% of the basin's population and produce more than 85% of the basin's GDP. Hence, subsequent socioeconomic exposures to flood intensity were the highest in these regions, with population

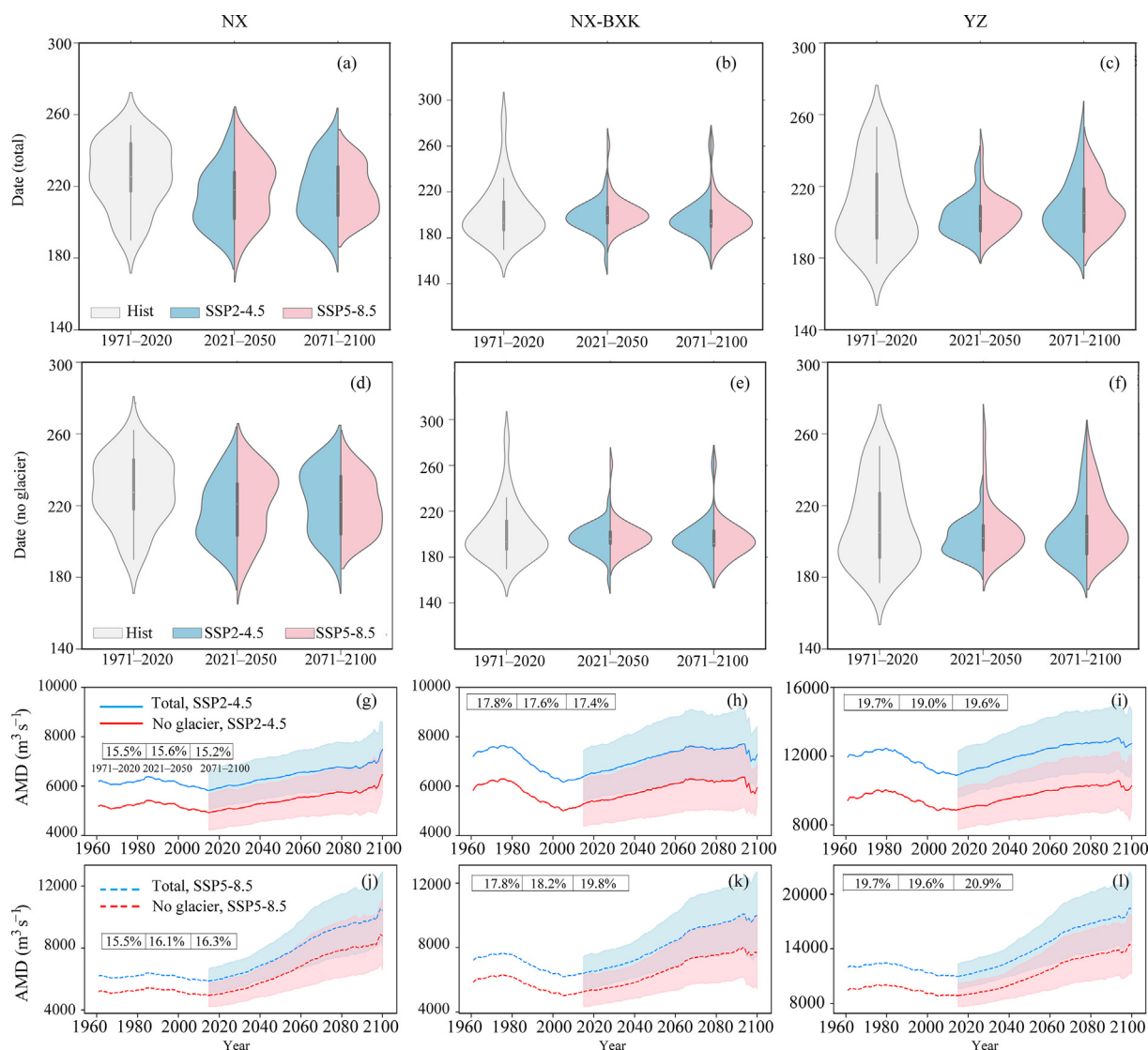


Fig. 5. (a–f) The occurrence date of annual maximum daily streamflow (AMD) with and without glacier runoff in the YZ basin and its two sub-basins, (g–l) simulated AMD with and without including glacier runoff in the YZ basin and its two sub-basins, with 30-year moving windows from 1961 to 2100 under each SSP (The numbers in each panel are the contribution of glacier runoff to mean annual AMD in the history and future periods, respectively).

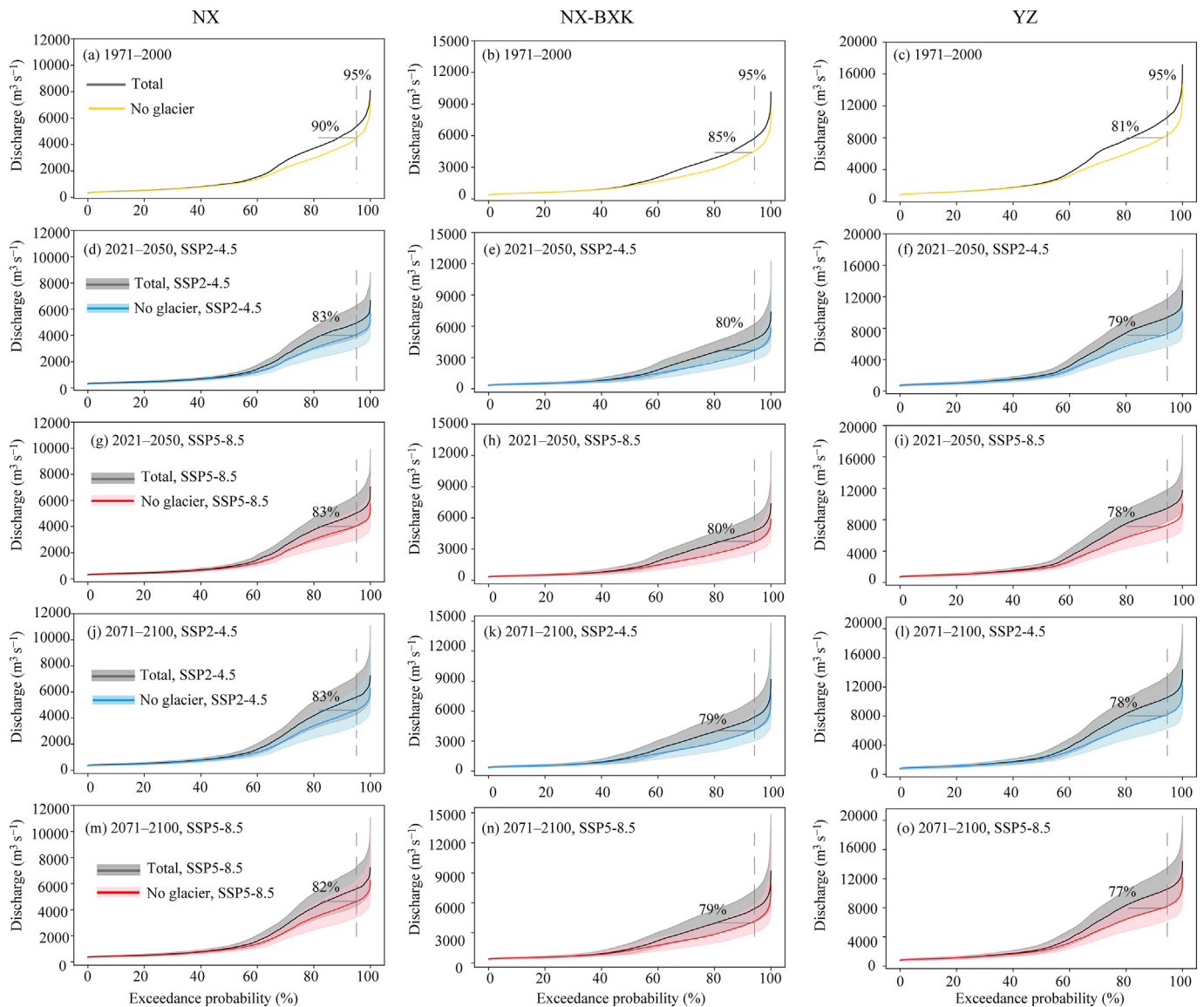


Fig. 6. Flow duration curves for simulated daily runoff with and without glacier melt under SSP2-4.5 and SSP5-8.5 during 2021–2050 and 2071–2100 in the YZ basin and its NX and NX-BXK sub-basins (The solid lines for the projection periods indicate the ensemble means of all transient simulations. Shadings denote the standard deviation of 10 hydrological model runs driven by different climate models).

(GDP) exposure to floods of 8–12 million persons (33–50 billion CNY, Fig. A2). The spatial pattern of the effect of glacier melt on flood intensity (Fig. A1), the difference between the simulated annual maximum daily discharge with and without glacier melt (Fig. A1), was similar to the spatial pattern of glacier distribution (Fig. 7a), with the strongest (10,000–35,000  $\text{m}^3 \text{s}^{-1}$ ) in the NX-BXK sub-basin (Fig. 7b). The glacier contribution to flood-subsequent population exposures was approximately 6%–8% (0.4–0.9 million people) in the YZ basin in 2071–2100 under the SSP5-8.5, and 10%–13% (1.0–1.6 million people) in the middle and downstream sub-basin (Fig. A2). The GDP exposures were approximately 2%–5% (0.7–2.5 billion CNY) in the YZ basin, and 7%–8% (2.3–3.3 billion CNY) in the downstream sub-basin in 2071–2100 under the SSP5-8.5 (Fig. 7c). In summary, the influence of glacier runoff on flood-subsequent socioeconomic

exposures was limited, mostly due to the low contribution of glacier runoff and the small population and the GDP in the glacier regions. It was gradually offset by precipitation-induced flooding from glacier areas to downstream regions.

## 5. Limitations and implications

This study highlights the effect of glacier melt on future extreme floods in the YZ basin based on a well-validated large-scale glacier-hydrology model. Generally, tipping point of glacier runoff played important roles in flood timing and intensity, especially in melt-dominated basins. However, existing studies on tipping points have shown some uncertainties in the YZ basin. Huss and Hock (2018) suggested that glacier runoff was projected to continue to rise until  $2030 \pm 18$  to  $2049 \pm 30$  in the Brahmaputra basin. Rounce

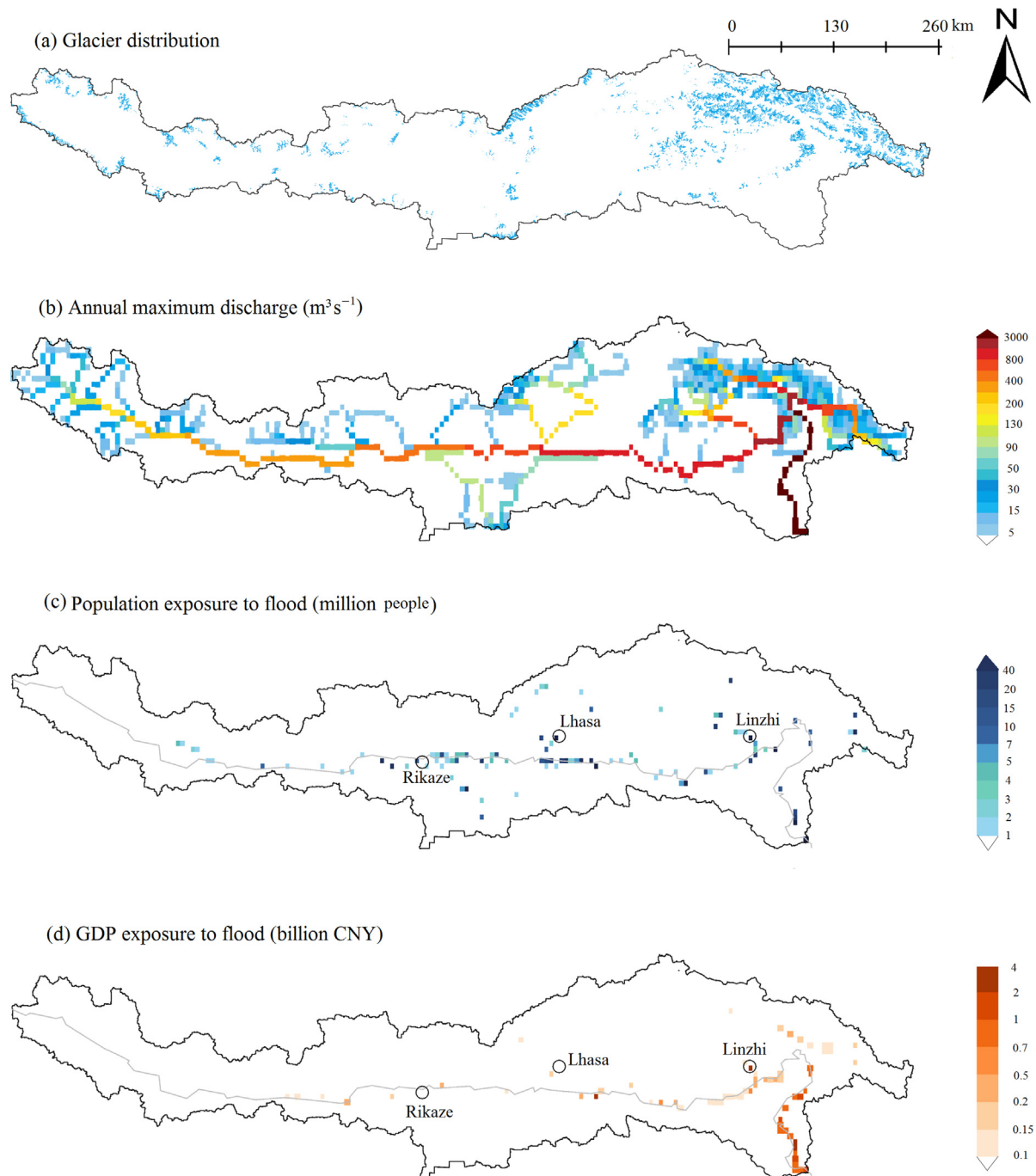


Fig. 7. Simulated spatial pattern of glacier coverage, annual maximum discharge of glacier melt, and exposure of population and GDP to annual maximum discharge of glacier melt in the YZ basin based on the ensemble mean of 10 transient runs in 2071–2100 under the SSP5-8.5.

et al. (2020) suggested that all southeast Asia basins (e.g., Ganges and Brahmaputra) will reach the tipping point of glacier runoff by 2050 for all emission scenarios. The differences primarily stemmed from uncertainties regarding forcing inputs and the glacier-hydrological process. The ranges in future climate projections were highly related to historical forcing inputs, which were the basis for bias correction of the GCMs. The degree day algorithm is a feasible way to simulate glacier melt due to its simplicity and effectiveness (Hock, 2003). However, the degree-day factor (DDF) was major

source of uncertainty, which largely relied on the initial glacier condition. Su et al. (2022) suggested that glacier runoff increased approximately 1.3%–3.2% when the DDF changed by one unit ( $\text{mm } ^\circ\text{C}^{-1} \text{d}^{-1}$ ) over the western TP basins. Therefore, more available observations of meteorological data and mass balance data in the glacier area are needed to develop a better description of glacier-hydrological processes in the large-scale basins of the TP. In addition to the uncertainties in the glacier model, additional uncertainties were introduced in the model representation of flood processes. In

this work, flood defence infrastructure, such as reservoirs, was not considered, and thus the estimated exposure could be considered as the potential flood risk.

As an important international river, the YZ-Brahmaputra River sustains the lives of approximately 70 million people (Immerzeel et al., 2010). The Brahmaputra River basin, with its large population and agricultural areas in the delta's floodplain, is at serious risk of extreme floods (Wijngaard et al., 2017). Improving the flood protection level and increasing investment in reservoir construction would be adaptive and responsive strategies. Yun et al. (2021) suggested that a reservoir with a total storage capacity of 100.3 km<sup>3</sup> could mitigate basin-wide future wet extremes by approximately 6%–32%. However, there was only one reservoir (<http://globaldamwatch.org>), mostly used for power generation, in the middle stream region of the YZ, and no reservoirs in the downstream sub-basin, which is the most severe region for extreme floods. The biggest problem was the costs and challenges involved in building infrastructure in such a high mountainous region. Fortunately, water stress issues in this region have been recognized by the Chinese government, and some risk responses and projects are currently being employed.

Here, we used the YZ basin as a projection framework example to help enrich the understanding of future flood changes and risks in rainfall or meltwater-impacted basins across the TP. The aforementioned scientific questions and limitations were also generally noted in melt-dominated basins of the TP, such as the upper Indus and Tarim River basins. The effect of glacier melt on extreme flooding in these basins was stronger than that in the YZ basin, mostly due to its greater glacier coverage and its glacier contributions to total runoff (Su et al., 2022). This suggests the advantage of international cooperation in flood risk management by systematically and comprehensively utilizing multiple disciplines of researchers and study methods from different countries.

## 6. Conclusions

Using a well-validated large-scale glacier-hydrology model, we extensively measured the future progression of extreme flooding and the impact of glacier melt on alterations in extreme floods during the 21st-century under the SSP2-4.5 and SSP5-8.5. Our main findings are summarized below.

- (1) The extreme flood, which was mainly reflected by in the duration and intensity, increased throughout the 21st-century, with greater rates of increase in the latter half of the century for SSP5-8.5. But regional differences in the characteristics of flood changes occurred between the NX and NX-BXK sub-basins of the YZ basin, with higher intensity and frequency, and shorter duration in the NX-BXK, and the opposite in the NX sub-basin.
- (2) Glacier runoff was projected to increase (2–30 mm per decade) throughout the 21st century, but there was also a noticeable decline or deceleration during the first half of

the century under SSP2-4.5, and in the latter half of the 21st century under SSP5-8.5. Glacier melt was projected to enhance the duration (12%–23%) and intensity (15%–21%) of extreme floods under both SSPs in the YZ basin, which would amplify the effects of future flooding on socioeconomics.

## Declaration of competing interest

The authors declare no conflict of interest.

## CRediT authorship contribution statement

He Sun: Conceptualization, Data curation, Formal analysis, Funding acquisition, Investigation, Methodology, Project administration, Resources, Software, Supervision, Validation, Visualization, Writing – original draft, Writing – review & editing. Tan-Dong Yao: Conceptualization, Funding acquisition, Resources, Visualization. Feng-Ge Su: Investigation, Methodology, Writing – review & editing. Tinghai Ou: Methodology, Writing – review & editing. Zhihua He: Methodology, Writing – review & editing. Guoqiang Tang: Methodology, Writing – review & editing. Deliang Chen: Writing – review & editing.

## Acknowledgments

This study was financially supported by the National Natural Science Foundation of China (42201140) and project funded by China Postdoctoral Science Foundation (2022M723256).

## Appendix A. Supplementary data

Supplementary data to this article can be found online at <https://doi.org/10.1016/j.accre.2024.01.003>.

## References

- AghaKouchak, A., Chiang, F., Huning, L.S., et al., 2020. Climate extremes and compound hazards in a warming world. *Annu. Rev. Earth Planet Sci.* 48 (1), 519–548. <https://doi.org/10.1146/annurev-earth-071719-055228>.
- An, B., Wang, W., Yang, W., et al., 2021. Process, mechanisms, and early warning of glacier collapse-induced river blocking disasters in the Yarlung Tsangpo Grand Canyon, southeastern Tibetan Plateau. *Sci. Total Environ.* 816, 151652. <https://doi.org/10.1016/j.scitotenv.2021.151652>.
- Belloni, R., Camici, S., Tarpanelli, A., 2021. Towards the continuous monitoring of the extreme events through satellite radar altimetry observations. *J. Hydrol.* 603, 126870. <https://doi.org/10.1016/j.jhydrol.2021.126870>.
- Boulange, J., Hanasaki, N., Yamazaki, D., et al., 2021. Role of dams in reducing global flood exposure under climate change. *Nat. Commun.* 12 (1), 417. <https://doi.org/10.1038/s41467-020-20704-0>.
- Cigizoglu, H.K., Bayazit, M., 2000. A generalized seasonal model for flow duration curve. *Hydrol. Process.* 14 (6), 1053–1067. [https://doi.org/10.1002/\(sici\)1099-1085\(20000430\)14:6<1053::Aid-hyp996>3.0.Co;2-b](https://doi.org/10.1002/(sici)1099-1085(20000430)14:6<1053::Aid-hyp996>3.0.Co;2-b).
- Eyring, V., Bony, S., Meehl, G.A., et al., 2016. Overview of the coupled model Intercomparison project Phase 6 (CMIP6) experimental design and organization. *Geosci. Model Dev. (GMD)* 9 (5), 1937–1958. <https://doi.org/10.5194/gmd-9-1937-2016>.

- Hirabayashi, Y., Mahendran, R., Koirala, et al., 2013. Global flood risk under climate change. *Nat. Clim. Change* 3 (9), 816–821. <https://doi.org/10.1038/nclimate1911>.
- Hoang, L.P., Lauri, H., Kummu, M., et al., 2016. Mekong River flow and hydrological extremes under climate change. *Hydrol. Earth Syst. Sci.* 20 (7), 3027–3041. <https://doi.org/10.5194/hess-20-3027-2016>.
- Hock, R., 2003. Temperature index melt modelling in mountain areas. *J. Hydrol.* 282 (1–4), 104–115. [https://doi.org/10.1016/s0022-1694\(03\)00257-9](https://doi.org/10.1016/s0022-1694(03)00257-9).
- Huss, M., Hock, R., 2018. Global-scale hydrological response to future glacier mass loss. *Nat. Clim. Change* 8 (2), 135–140. <https://doi.org/10.1038/s41558-017-0049-x>.
- Immerzeel, W.W., van Beek, L.P., Bierkens, M.F., 2010. Climate change will affect the Asian water towers. *Science* 328 (5984), 1382–1385. <https://doi.org/10.1126/science.1183188>.
- Li, Y., Wang, C., Su, F., 2021. Evaluation of climate in CMIP6 models over two Third Pole subregions with contrasting circulation systems. *J. Clim.* 34 (22), 9133–9152. <https://doi.org/10.1175/jcli-d-21-0214.1>.
- Liang, X., Lettenmaier, D.P., Wood, E.F., et al., 1994. A simple hydrologically based model of land-surface water and energy fluxes. *J. Geophys. Res. Atmos.* 99 (D7), 14415–14428. <https://doi.org/10.1029/94jd00483>.
- Lutz, A.F., Immerzeel, W.W., Kraaijenbrink, P.D., et al., 2016. Climate change impacts on the upper indus hydrology: sources, shifts and extremes. *PLoS One* 11 (11), e0165630. <https://doi.org/10.1371/journal.pone.0165630>.
- Lutz, A.F., Immerzeel, W.W., Siderius, C., et al., 2022. South Asian agriculture increasingly dependent on meltwater and groundwater. *Nat. Clim. Change* 12 (6), 566–573. <https://doi.org/10.1038/s41558-022-01355-z>.
- Rounce, D.R., Hock, R., Shean, D.E., 2020. Glacier mass change in High Mountain Asia through 2100 using the open-source Python Glacier evolution model (PyGEM). *Front. Earth Sci.* 7, 331. <https://doi.org/10.3389/feart.2019.00331>.
- Shao, X., Zhang, Y., Ma, N., et al., 2023. Flood increase and drought mitigation under a warming climate in the southern Tibetan Plateau. *J. Geophys. Res. Atmos.* 128 (2), e2022JD037835. <https://doi.org/10.1029/2022jd037835>.
- Su, F., Zhang, L., Ou, T., et al., 2016. Hydrological response to future climate changes for the major upstream river basins in the Tibetan Plateau. *Global Planet. Change* 136, 82–95. <https://doi.org/10.1016/j.gloplacha.2015.10.012>.
- Su, F., Pritchard, H.D., Yao, T., et al., 2022. Contrasting fate of western Third Pole's water resources under 21st century climate change. *Earth's Future* 10 (9), e2022EF002776. <https://doi.org/10.1029/2022ef002776>.
- Sun, H., Su, F., 2020. Precipitation correction and reconstruction for streamflow simulation based on 262 rain gauges in the upper Brahmaputra of southern Tibetan Plateau. *J. Hydrol.* 590, 125484. <https://doi.org/10.1016/j.jhydrol.2020.125484>.
- Sun, H., Su, F., He, Z., et al., 2021. Hydrological evaluation of high-resolution precipitation estimates from the WRF model in the Third Pole river basins. *J. Hydrometeorol.* (8), 2055–2071. <https://doi.org/10.1175/jhm-d-20-0272.1>.
- Sun, H., Yao, T., Su, F., He, Z., et al., 2022. Corrected ERA5 precipitation by machine learning significantly improved flow simulations for the Third Pole basins. *J. Hydrometeorol.* 23 (10), 1663–1679. <https://doi.org/10.1175/JHM-D-22-0015.1>.
- Thrasher, B., Maurer, E.P., McKellar, C., et al., 2012. Technical note: bias correcting climate model simulated daily temperature extremes with quantile mapping. *Hydrol. Earth Syst. Sci.* 16 (9), 3309–3314. <https://doi.org/10.5194/hess-16-3309-2012>.
- Wang, Y., Wang, L., Zhou, J., et al., 2021. Vanishing glaciers at southeast Tibetan Plateau have not offset the declining runoff at Yarlung Zangbo. *Geophys. Res. Lett.* 48 (21), e2021GL094651. <https://doi.org/10.1029/2021gl094651>.
- Wang, Y., Cui, P., Zhang, C., et al., 2024. Antecedent snowmelt and orographic precipitation contributions to water supply of Pakistan disastrous floods. *Adv. Clim. Change Res.* 2022. <https://doi.org/10.1016/j.accre.2023.12.002>.
- Wijngaard, R.R., Lutz, A.F., Nepal, S., et al., 2017. Future changes in hydroclimatic extremes in the upper indus, Ganges, and Brahmaputra River basins. *PLoS One* 12 (12), e0190224. <https://doi.org/10.1371/journal.pone.0190224>.
- Wood, A.W., 2002. Long-range experimental hydrologic forecasting for the eastern United States. *J. Geophys. Res. Atmos.* 107 (D20). <https://doi.org/10.1029/2001jd000659>. ACL 6-1-ACL 6-15.
- Wood, A.W., Leung, L.R., Sridhar, V., et al., 2004. Hydrologic implications of dynamical and statistical approaches to downscaling climate model outputs. *Climatic Change* 62 (1–3), 189–216. <https://doi.org/10.1023/B:CLIM.0000013685.99609.9e>.
- Xiao, C., Zhang, T., Che, T., et al., 2023. Do abrupt cryosphere events in High Mountain Asia indicate earlier tipping point than expected? *Adv. Clim. Change Res.* 14 (6). <https://doi.org/10.1016/j.accre.2023.11.006>.
- Yang, L., Li, K., Shen, Y., et al., 2022. Flood seasonality over the Third Pole region modulated by upper level moisture transport. *Earth's Future* 10 (9), e2022EF002828. <https://doi.org/10.1029/2022ef002828>.
- Yao, T., Thompson, L., Yang, W., et al., 2012. Different glacier status with atmospheric circulations in Tibetan Plateau and surroundings. *Nat. Clim. Change* 2 (9), 663–667. <https://doi.org/10.1038/nclimate1580>.
- Yun, X., Tang, Q., Li, J., et al., 2021. Can reservoir regulation mitigate future climate change induced hydrological extremes in the Lancang-Mekong River basin? *Sci. Total Environ.* 785, 147322. <https://doi.org/10.1016/j.scitotenv.2021.147322>.
- Zhang, L., Su, F., Yang, D., et al., 2013. Discharge regime and simulation for the upstream of major rivers over Tibetan Plateau. *J. Geophys. Res. Atmos.* 118 (15), 8500–8518. <https://doi.org/10.1002/jgrd.50665>.
- Zhou, Y., 2020. Exploring multidecadal changes in climate and reservoir storage for assessing nonstationarity in flood peaks and risks worldwide by an integrated frequency analysis approach. *Water Res.* 185, 116265.